



Evaluation of the bifaciality coefficient of bifacial photovoltaic modules under real operating conditions

E. Muñoz-Cerón^{a,b,*}, S. Moreno-Buesa^b, Jonathan Leloux^c, J. Aguilera^b, David Moser^d

^a Division of Projects Engineering, Department of Graphic Engineering, Design and Projects, University of Jaén, Spain

^b PV IDEA Research Group (Research and Development in Solar Energy), Centre for Advanced Studies in Earth Science, Energy and Environment, University of Jaén, Spain

^c LuciSun, Sart-Dames-Avelines, Belgium

^d EURAC Research, Bolzano, Italy

ARTICLE INFO

Handling Editor: Panos Seferlis

Keywords:

Bifacial
Photovoltaic
Bifaciality
Outdoors

ABSTRACT

Among the parameters that define a bifacial photovoltaic module, the bifaciality coefficients indicate the rear and front side ratio of the most representative IV curve points of a photovoltaic panel, that is, I_{sc} , V_{oc} and P_m . However, these parameters are defined under the ideal Standard Test Conditions (STC). Therefore, to provide a realistic insight regarding the performance of bifacial modules, it is necessary to evaluate these coefficients under real operating conditions. For such purpose, an outdoor campaign was performed to experimentally measure the maximum power bifaciality coefficient of two modified bifacial modules that resemble a rear and a front monofacial panel respectively. As a first result, if the measurements are translated to STC, using a linear approximation, the bifaciality matches the value indicated by the manufacturer. Additionally, the operating bifaciality coefficient shows a linear decrease trend, proportional to the irradiance level decrease. This result implies that on cloudy days, the average bifaciality factor is below the corresponding one from sunny days. Finally, for irradiances below 200 W/m^2 , there is a non-linear increase in the bifaciality, with greater values than the corresponding to the ideal STC conditions, which presumably are caused by the non-linearity performance of photovoltaic modules at low irradiances.

1. Introduction

The use of bifacial photovoltaic (PV) systems and their scientific study, can be traced back to the 1980s (Eguren et al., 2022). During this period, pioneering research, such as the work conducted by Cuevas et al., in 1982, involved experimental analysis to explore the potential benefits of bifacial modules in relation to albedo, and compared these gains with those of conventional panels (Cuevas et al., 1982).

However, in recent years this technology has experienced an exponential market growth rate, and it is expected to become the main predominant technology in new PV installations in the coming years (VDMA, 2022).

Within this context, a considerable body of scientific literature has emerged, encompassing diverse facets of bifacial modules. Notably, a multitude of articles delve into the examination of potential advantages achieved through the integration of solar trackers (Patel et al., 2021; Rodríguez-Gallegos et al., 2020; Yakubu et al., 2022). In addition,

several studies show possible bifacial applications, ranging from integration in buildings (Tina et al., 2021b) or roofs (Muehleisen et al., 2021), and other infrastructures such as noise barriers (Nordmann and Clavadetscher, 2004) or even floating PV installations (Tina et al., 2021a). The use of bifacial modules in agricultural sites, the so-called agrivoltaic systems, also entails another application with great potential (Katsikogiannis et al., 2022), especially on vertically mounted installations (Chudinow et al., 2020; Riaz et al., 2021).

Numerous studies experimentally address the unknowns that still exist regarding the operation and performance of this technology. Some of them cover a broader scope, conducting outdoor tests (Gu et al., 2021), whereas other studies delve into more intricate assessments, comparing the performance of fixed systems, trackers, and the impact of varying albedo on PV module efficiency (Riedel-Lyngskær et al., 2020).

A significant volume of experimental studies focus on the analysis of the incident irradiance on the back side of these modules, where irradiance maps depending on the positioning of the PV panels have been

* Corresponding author. Division of Projects Engineering, Department of Graphic Engineering, Design and Projects, University of Jaén, Spain.
E-mail address: emunoz@ujaen.es (E. Muñoz-Cerón).

graphed (Riedel-Lyngskaer et al., 2020). These variations in the back-side energy capture can produce mismatch losses that need to be parameterized (Tao et al., 2021).

The objective of these studies is to provide tools that allow scientists to characterise the bifacial modules under the variable operating conditions prevailing outdoors (Kenny et al., 2018). This knowledge may enable the development of more appropriate energy and power rating procedures for bifacial photovoltaic modules (Vogt et al., 2023).

However, overall, the experimental knowledge regarding the operation, performance and characterization of this technology is not enough. There is a general lack of experiments performed outdoors, especially those that analyse parameters beyond the expected energy gains in these bifacial modules or mismatch between them. Moreover, there is a necessity to deal with the influence of environmental conditions on some specific parameters of bifacial modules operation, such as the bifaciality coefficient.

In a context of great industrial deployment and relevant scientific production covering this technology, experts have also met to define a common frame of reference at the normative level within the International Electrotechnical Commission, although, to date, only five international standards mention or directly cover aspects of the bifacial technology.

The last version of the IEC 61215-1 and IEC 61215-2 standards, which date from 2021, include definitions, references and instructions on how to perform the design qualification and type approval on bifacial PV modules ((IEC) International Electrotechnical Commission, 2021a) and it contains the test methods required for these bifacial modules ((IEC) International Electrotechnical Commission, 2021b).

The IEC TS 63202–3:2023 standard describes the procedure for the measurement of current-voltage (I–V) characteristics of unencapsulated bifacial photovoltaic cells for indoor applications, that is, laboratories or assembly lines production ((IEC) International Electrotechnical Commission, 2023).

The measurement of this IV curve, in natural or simulated sunlight, but applied to photovoltaic bifacial modules, adheres to the technical specification IEC TS 60904-1-2:2019. It describes the procedure to measure, under Standard Test Conditions, the IV characteristics of the rear and front side of the bifacial module independently, that is, that the rear side cannot interfere in the response of the measured front side of the module and vice versa ((IEC) International Electrotechnical Commission, 2019).

The measurement procedure proposed in the aforementioned standard enables us to define the bifaciality coefficients, which they are also mentioned in the IEC 61724–1:2021 standard. These parameters indicate the rear and the front side ratio of the most representative points of the IV characteristics of the bifacial module. Consequently, each bifacial module should inherently exhibit three fundamental values: bifaciality coefficient of I_{sc} (φ_{Isc}), V_{oc} (φ_{Voc}) and P_m (φ_{Pmax}), respectively. Nevertheless, manufacturers mostly indicate solely the corresponding coefficient concerning the ratio between maximum powers of both sides (φ_{Pmax}) ((IEC) International Electrotechnical Commission, 2021c).

Several scientific references have explored the implementation of the TS 60904-1-2:2019, in which they have identified the advantages and disadvantages, together with the feasibility, to undertake the tests indicated in these norms. They highlighted that the rear-side non-uniformity requirements are complicated to fulfil in outdoor testing (Kenny et al., 2018; Lopez-Garcia et al., 2022).

In addition, the IEA PVPS Task 13 also identified a lack of consensus to define the nominal power of PV modules. The majority of the manufacturers only use the STC maximum power of the front side, as prescribed by the IEC 61724–1:2021. They ignore the contribution of the rear side and the definition of bifacial nameplate irradiance (BNPI). Moreover, besides this lack of reference conditions for the rated output power, there are no requirements concerning the incorporation of the bifacial parameters in the module's datasheet (IEA PVPS Task 13, 2021). For the design of the safety requirements of BF systems (e.g. overcurrent

protection), the rating must be evaluated for I_{sc} at BSI (Bifacial Stress Irradiance), where it is applied an irradiance of 1000 W/m^2 in the front side and 300 W/m^2 in the rear side, or what is declared by the manufacturer, as prescribed by the 61730-1 (edition 3), which was recently published in September 2023.

Another limitation is that the bifacial coefficients are defined under the ideal Standard Test Conditions (STC). However, it is also necessary to evaluate them under operating conditions in order to provide realistic information regarding the performance of bifacial modules, with the aim of reducing the gap between any standards based on ideal conditions and tests performed under a real operating scenario.

The bifaciality coefficients are one of the key parameters to consider in the design of PV systems using bifacial technology, and there are numerous publications related to the bifaciality factor, but all of them from a design approach at cell level. In the literature review, one publication deals with the impact that this parameter could have on the normalized cost of electricity generated with the bifacial technology (Libal, 2018). However, there is only one publication that investigates the variation of the bifaciality coefficient under different irradiance levels, but it refers to a module manufactured specifically for this experiment which was tested indoors and at irradiance levels higher than 700 W/m^2 (Bai et al., 2021).

According to the published literature regarding the outdoor characterization of the performance of bifacial technology and, to the best of our knowledge at the time of publication, there is a knowledge gap related to the analysis and evaluation of the bifaciality coefficients under real operating conditions.

Therefore, the output of the research described in our work aims to further deepen in the knowledge of the bifacial technology, and to reduce the existing gap between the results obtained under simulations or experimental measurements conducted under controlled test conditions (indoor) and those existing outdoors.

According to the previous findings, the motivation of this manuscript lies in overcoming the scarcity of experimental knowledge regarding the operation, performance and characterization of the bifacial technology based on real outdoor conditions. It may enable us to assess the influence of environmental conditions on some specific parameters of bifacial modules operation, such as the bifaciality coefficient, which it is not sufficiently covered in the scientific literature. In addition, the motivation also lies in overcoming the experimental gap between any standards based on ideal conditions and tests performed under real operating conditions.

Therefore, the main novelty of this work lies in the evaluation of the bifaciality coefficient of a conventional and market available bifacial module, but instead of by means of a simulation or indoor characterisation, based on real outdoor conditions.

This manuscript, which aims to contribute to the evaluation of the maximum power bifaciality coefficient under real outdoors conditions, is structured as follows. Section 2 describes the experimental set-up that has enabled the proposed research to be carried out through the methodology explained in this section. The results and their discussion are presented in Section 3. The conclusions, limitation and future works are detailed in Section 4.

2. Experimental set-up and methodology

2.1. – description of the set-up and the measurement campaign

For the evaluation of the bifaciality coefficient of bifacial photovoltaic (BFPV) modules under real operating conditions, an experimental set-up was installed in the outdoor laboratory facilities of the IDEA PV research team, located in Jaén, Spain (coordinates: 37.78° , -3.79°). Fig. 1 shows this experimental set-up and it also indicates the modules selected for the analysis. In addition, Fig. 2 allows identifying the slight modification made to the bifacial module to convert it into a monofacial one. In this case, the front-side was covered and the module was turned



Fig. 1. Experimental set-up for the outdoors evaluation of the bifacial coefficient.

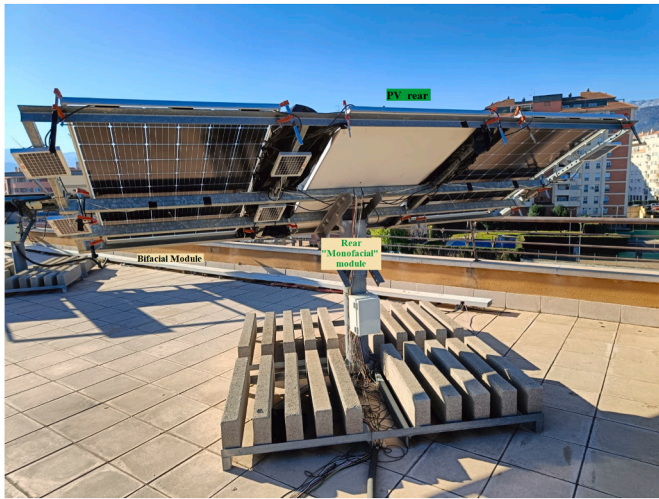


Fig. 2. Rear view of the experiment with the bifacial module (PV_rear) covered on one side (middle module).

upside down.

The procedure used for this evaluation consisted in comparing the performance of two bifacial modules from the same manufacturer, model, and batch, which are operating individually at their respective maximum power point by means of power optimisers. Specifically, these modules are framed glass-glass panels composed of 60 N-type crystalline silicon solar cells.

The modules have a 290 W front-side rated power at standard test conditions (STC: $G = 1000 \text{ W/m}^2$, $T_c = 25 \text{ }^\circ\text{C}$, $AM1.5G$). In addition, the technical characteristics are also indicated under a Bifacial Standard Test Conditions (BSTC), defined by the manufacturer, which correspond to Irradiance: $1000 \text{ W/m}^2 + \text{Min}(\varphi_{Isc}, \varphi_{Pm}) \cdot 135 \text{ W/m}^2$; $25 \text{ }^\circ\text{C}$ cell temperature and $AM1.5G$ spectrum according to EN 60904-3, where φ_{Isc} , φ_{Pm} stands for the bifaciality coefficient defined for short-circuit current and maximum power respectively. These technical characteristics are summarised in Table 1.

Due to the lack of consensus to define the nominal power of bifacial PV modules, the manufacturer of the modules under test followed the specifications from the TÜV Rheinland, which proposes a specific bifacial standard test conditions of 1000 W/m^2 front-side and 135 W/m^2 rear-side irradiance respectively (Herrmann et al., 2017; IEA PVPS Task 13, 2021). The new version of the IEC 61215:2021 also considers these specifications, referred to as Bifacial Nameplate Irradiance ((IEC) International Electrotechnical Commission, 2021a).

The thermal characteristics of the bifacial PV modules under test and the bifaciality coefficients are indicated in Table 2.

Table 1

Technical characteristics of the bifacial module indicated in the datasheet of the manufacturer.

	Standard Test Conditions (STC)	Bifacial Standard Test Conditions (BSTC)
Peak Power, P_m (W)	290	320
Voltage at P_m , V_{mpp} (V)	32.3	32.3
Current at P_m , I_{mpp} (A)	8.98	9.97
Open-Circuit Voltage, V_{oc} (V)	39.2	39.2
Short-Circuit Current, I_{sc} (A)	9.34	10.36

Table 2

Thermal Characteristics of the bifacial module as indicated in the datasheet of the manufacturer.

Nominal module operating temperature	NMOT ($^\circ\text{C}$)	39 ± 2
Temperature coefficient (P_m)	γ_{Pm} ($\%/^\circ\text{C}$)	-0.38
Bifaciality (P_m)	φ_{Pm} (%)	82.0
Temperature coefficient (V_{oc})	β_{Voc} ($\%/^\circ\text{C}$)	-0.30
Bifaciality (V_{oc})	φ_{Voc} (%)	99.3
Temperature coefficient (I_{sc})	α_{Isc} ($\%/^\circ\text{C}$)	0.04
Bifaciality (I_{sc})	φ_{Isc} (%)	81.5

In order to assess the difference between the characteristic from the technical data sheet and the particular data of each module, the flash-list data provided by the manufacturer, measured under BSTC, is also indicated in Table 3. Module 1 corresponds to the panel named PV_front in Fig. 1, while module 2 corresponds to the panel named PV_rear. This information is useful to assess that their performance are very similar. In the flash list report, the manufacturer does not provide any information regarding the bifaciality coefficient of these modules.

The bifacial modules under test were arranged in two parallel structures, with the same orientation and inclination (South oriented and tilted 30°), as Fig. 1 shows. The support structures are straight and robust enough to keep the verified initial conditions unchanged.

In order to assess and analyse the bifaciality factor performance, operating under real outdoors conditions, the devices under tests were modified so their operation resembles a monofacial module. This modification was applied to different sides of the modules. The photovoltaic module denominated ‘‘PV_front’’ is a bifacial panel whose rear side was covered with an opaque vinyl coating and the front face is the one exposed to the sun. Thus, it behaves as a conventional monofacial module. On the other hand, the front side of the second module under test (‘‘PV_rear’’) was covered with the same opaque vinyl coating (see Fig. 2), and the module was turned upside-down. Therefore, its rear side was the one exposed to the incident front irradiance and the front-side of this second module, which is covered, was facing the ground. Despite the ‘‘PV_rear’’ arrangement corresponds to the contrary of the usual

Table 3

Flash list of the bifacial modules under test measured at BSTC.

	Module 1: PV_Front	Module 2: PV_Rear	Mod 2 vs Mod 1 differences (%)
Peak Power, $P_{m_{BSTC}}$ (W)	324.37	324.46	0.03
Voltage at $P_{m_{BSTC}}$, $V_{mpp_{BSTC}}$ (V)	31.89	31.51	-1.21
Current at $P_{m_{BSTC}}$, $I_{mpp_{BSTC}}$ (A)	10.17	10.29	+1.26
Open-Circuit Voltage, $V_{oc_{BSTC}}$ (V)	38.97	38.96	-0.03
Short-Circuit Current, $I_{sc_{BSTC}}$ (A)	10.71	10.79	0.6

positioning for these modules, it will enable us to conduct the analysis under the same incident irradiation conditions for both sides.

The inner layer of this opaque vinyl is black, in order to avoid incident light to be back scattered to the other side of the solar cells, thereby inducing internal reflections that could distort the results.

For the measurement of the operating conditions, the following devices were used: a reference photovoltaic module ($P_{m_{STC}} = 5 \text{ W}$) was used to measure the in-plane irradiance (POA). Previous works have shown that these reference modules present the best correlation to the reference cells (Riedel-Lyngskar et al., 2022). This reference irradiance sensor was calibrated against a pyranometer located in the same meteorological station (Model: Hukseflux SR20-T2) to assess the linear dependence of the short-circuit current and the incident irradiance of the modules used as sensors. T-type thermocouples were used to measure the ambient temperature and the temperature of both modules on their respective covered surfaces. All data registered within the experiment are synchronised.

The test procedure consisted of recording every 5 min, for almost one month, the maximum power of the two specimens under test, as well as the irradiance and temperature variables mentioned previously. Therefore, according to the standard IEC 61724-1, it corresponds to a Class A measurement system ((IEC) International Electrotechnical Commission, 2021c).

2.2. – data management and methodology

Initially, an unfiltered analysis of the measured data in relation to the meteorology was performed. Subsequently, in a further analysis, the data were aggregated and a differentiation between completely sunny days (clear-sky conditions), partially overcast, and days with predominant cloudiness was undertaken. This classification was established by visual inspection of the irradiance profiles.

Additionally, a temporal filter to analyse the performance of the bifaciality coefficient was applied, taking into account different time windows of the measurement days.

Finally, in later stages of the analysis, a discrimination according to irradiance levels was applied, differentiating between high irradiance values and irradiances below 200 W/m^2 . The manufacturer claims that this is the threshold where there is an average relative efficiency reduction of 1.9% according to the standard IEC 60904-10.

The methodology primarily involved evaluating the maximum power bifaciality coefficient, which was derived from the data recorded, according to the analyses mentioned above, to standard test conditions (STC).

It is possible to translate the measured operating power of the modules to the corresponding maximum power at Standard Test Conditions ($P_{m_{STC}}$) of both specimens, by the application of the following equation (Angulo et al., 2022; Muñoz et al., 2016):

$$\frac{P_m}{(1 + \gamma \cdot (T_c - T_{c_{STC}}))} = P_{m_{STC}} \cdot \frac{G}{G_{STC}} \quad (1)$$

Where P_m (W) is the operating maximum power recorded at each module, G (W/m^2) is the measured incident irradiance on the plane of the modules and T_c is the cell temperature ($^{\circ}\text{C}$), measured with thermocouples attached to each module. The temperature coefficient at maximum power (γ_{P_m} , $\%/^{\circ}\text{C}$) is the value indicated by the manufacturer in its datasheet (see Table 2). G_{STC} and $T_{c_{STC}}$ are the irradiance and cell temperature used to indicate the maximum power of the module at Standard Test Conditions ($P_{m_{STC}}$), which stands for $G_{STC} = 1000 \text{ W/m}^2$ and $T_{c_{STC}} = 25^{\circ}\text{C}$.

In the previous equation, the measured cell temperature has been corrected according to the values proposed by King et al. (2004).

The slopes of the linear fit of the above equation corresponds with the PV_rear and PV_front maximum powers at STC, and subsequently, the bifaciality coefficient of P_m (ρ_{P_m} or BF) under these ideal conditions

could be calculated and compared with the value indicated by the manufacturer.

Later on, the performance of this coefficient has been analysed, but under real operating conditions, with special emphasis on carrying out the study according to the existing day typology and different time windows. Finally, an evaluation of the dependence of the value of this coefficient on the existing irradiance levels was carried out.

3. Results and discussion

The experimental set-up recorded the modules' power throughout nearly one month in February 2023. In this time span, different types of days, in terms of climatological performance, have occurred, ranging from fully sunny to completely cloudy days. In this sense, the power output of the experiment could be grouped according to sunny days (clear-sky conditions), partially overcast, and days with predominant cloudiness. Figs. 3 and 4 show, for a representative sunny and cloudy day respectively, an example of the daily power output evolution of the modules under test during the experimental campaign. The power differences between the rear and front bifacial modules, due to the bifaciality factor defined previously, are noticeable.

The early and late hours of the day should be discarded due to the experimental set-up. In this case, as clearly observed in Fig. 3, nearby infrastructures can cast shadows on the modules, and thus the bifaciality results may not correspond to the reality, sometimes even resulting in bifaciality coefficients above 1. A filter corresponding to a threshold in Sun's Height of approximately 15° was applied. This is equivalent to eliminate 1.5 h of data at the beginning and the end of each day for both modules. A minimum irradiance threshold could not be considered, as it may mask the results corresponding to cloudy days.

3.1. – Maximum power bifaciality coefficient under standard test conditions

In order to obtain the power that the modules of the experimental set-up would have under STC conditions ($P_{m_{STC}}$), equation (1) was applied to each measured operating power, together with the modules' temperature and the incident in-plane irradiance. The slopes of the linear fit correspond with the rear and front module at STC respectively (see Fig. 5).

An initial analysis, where all the days of the experimental campaign were used, enables us to calculate the maximum power bifaciality coefficient under STC ($\rho_{P_m_{STC}}$), as Table 4 shows.

The result indicates that the value obtained practically matches the maximum power bifaciality coefficient stated by the manufacturer in the technical data sheet of the modules used, which amounts to 0.82.

However, the analysis of the complete set of recorded powers can be a source of distortion of the bifaciality coefficient result. For this reason, the same procedure as shown in Fig. 5 was repeated, but after grouping the days according to the weather conditions. In these cases, Table 4 also indicates the bifaciality coefficient at STC for sunny, partially overcast,

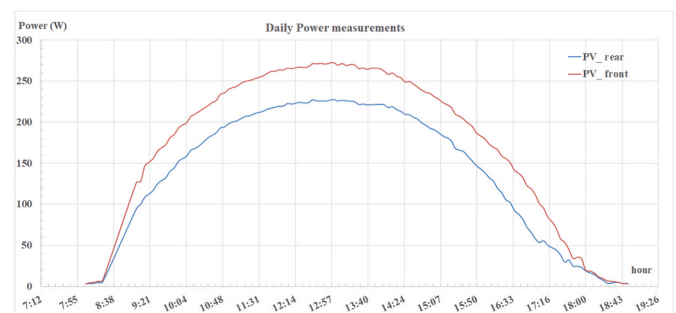


Fig. 3. Daily power outputs of the devices under test for a representative sunny day of the experiment.

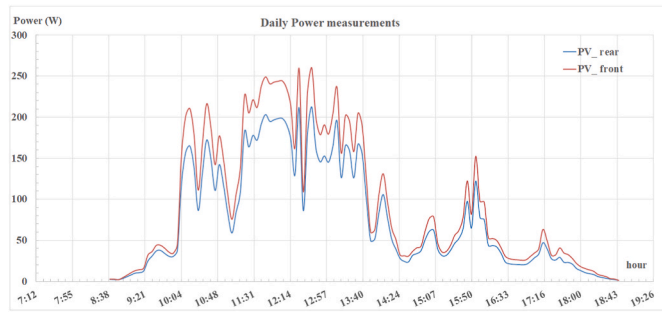


Fig. 4. Daily power outputs for a representative cloudy day of the experiment.

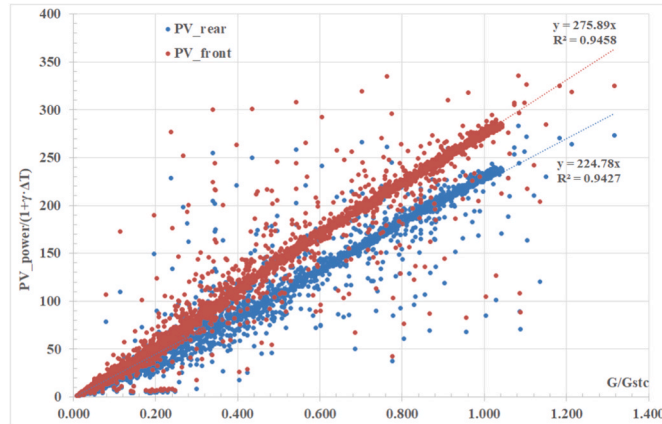


Fig. 5. Power output of the front and rear modules (The slope indicates the P_m at STC).

Table 4
Power Bifaciality results translated to STC.

	P_m PV_front (W)	R^2	P_m PV_rear (W)	R^2	STC Power Bifaciality $\rho_{P_m,STC}$
All days	276.21	0.919	225.25	0.916	0.816
Sunny days	277.96	0.994	226.69	0.979	0.816
Partially overcast days	278.05	0.936	226.65	0.942	0.815
Cloudy days	270.82	0.816	220.96	0.809	0.816

and cloudy days respectively.

Regardless of the existing daily meteorological variability or irradiance values of the samples, in all the cases shown in Table 4, the maximum power bifaciality factor translated to STC remains practically constant. However, if only the sunny days of the campaign are considered for the estimation of the maximum power bifaciality coefficient, the linear adjustment (R^2) is better.

This result proves that, as a first approximation and in order to obtain the maximum power bifaciality coefficient of the modules under STC, an outdoor characterization could be done with a certain independence of the meteorological variability.

3.2. – Maximum power bifaciality coefficient under real operating test conditions (OTC)

The result of the previous section does not necessarily imply that, regardless of the day, the maximum power bifaciality coefficient remains constant under real operating conditions.

According to the visual results of Figs. 3 and 4, the differences in the

operating power of the PV_front and PV_rear modules, and thus, in the bifaciality coefficient, apparently are not the same based on the sort of the day selected. Moreover, there is even some temporal variability depending on the time of the day analysed, especially on cloudy ones, so not even the bifaciality factor presumably remains constant throughout the daily temporary evolution.

For example, the power recordings of the PV_rear and PV_front modules corresponding to the representative example of sunny days (Fig. 3), indicate that the power bifaciality coefficient apparently remains constant at the central hours, whereas in the beginning and end of the day, these differences seem to slightly decrease (excluding the extremes values of the applied filter). On the other hand, in the case of a cloudy day (see Fig. 4), these rear and front power differences do not remain constant at any time throughout the day.

Fig. 6 shows a comparison of the temporal variation of the maximum power bifaciality coefficient (BF) under real operating test conditions for both representative days. The first noticeable difference is that, during the central hours of the recorded data, the bifaciality of the day classified as sunny remains approximately constant, whereas in the case of the result corresponding to the cloudy day, there is a greater variability in its temporal evolution.

The second difference shown in Fig. 6 is that, for the entire time range of these recordings, the average value of the bifaciality coefficient corresponding to the sunny day is slightly higher than the one corresponding to the day considered as cloudy or not stable. The mean daily value of the bifaciality coefficient is 0.809 for the sunny day, whereas it decreases down to 0.787 for the less stable cloudy day, which means a 2.76% difference for this particular comparison. It is noticeable that both values are lower than the maximum power bifaciality factor obtained under Standard Test Conditions in section 3.1.

It is important not to draw conclusions from the analysis of isolated days. However, Fig. 7 shows that the trend for the sunny days of the experimental campaign remains reasonably consistent across similar days.

On the other hand, Fig. 8 shows the time variation of the maximum power bifaciality factor for all the cloudy days of the experimental campaign. In this case, the bifaciality values are quite unstable compared to the results measured corresponding to the sunny days, and the variability throughout the day is greater than what it can be observed from Fig. 7. Nevertheless, all the measurements from these cloudy days may seem to follow a similar trend, that is, there are differences between the BF corresponding to central hours and those values from the edges of the day.

In order to corroborate the above-mentioned differences in the performance of the bifaciality coefficient under real operating conditions, depending on the type of day, this factor has been calculated considering not only the entire range of days measured, but also based on the classification of the existing type of day (see Table 5).

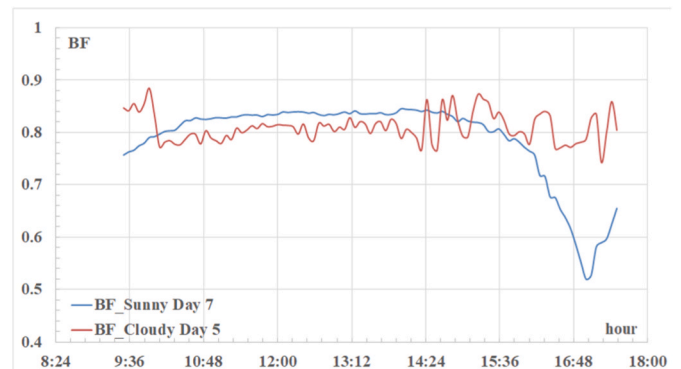


Fig. 6. Daily variation of the bifaciality coefficient for a representative sunny and a cloudy day.

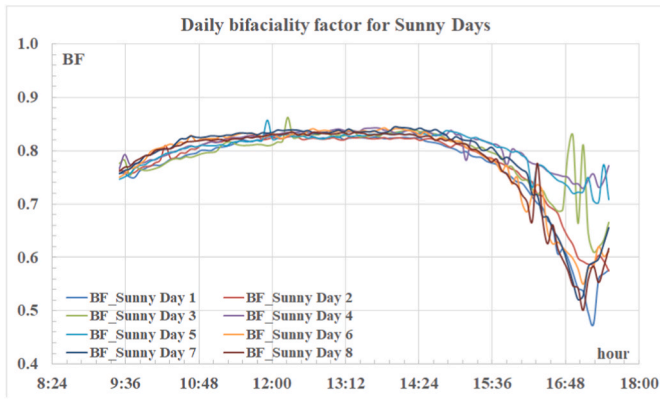


Fig. 7. Daily variation of the bifaciality coefficient for all sunny days of the experimental campaign.

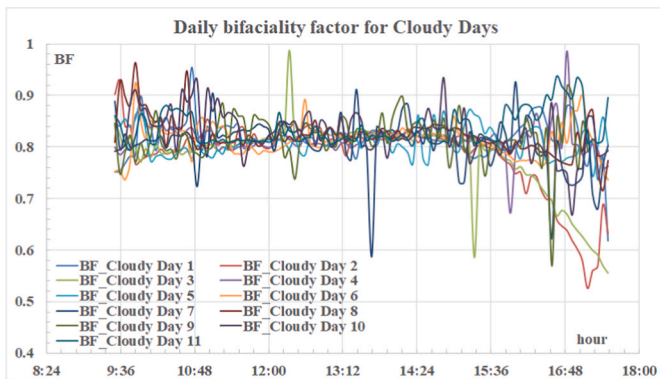


Fig. 8. Daily variation of the bifaciality coefficient for all cloudy days of the experimental campaign.

The first result is that in all cases, regardless of the type of day grouping, the average value of the bifaciality coefficient under OTC conditions is lower than that estimated under STC. The reason for this result is explained in Fig. 9, where the irradiance distribution of the different grouping of days is mostly below irradiances of 1000 W/m², which is the reference value to obtain $\rho_{PM,STC}$.

The results for the days classified as cloudy are also noteworthy. There is a relative difference with respect to $\rho_{PM,STC}$ that is lower than the average value obtained from the measurements collected on sunny days, despite the fact that the irradiance distribution distances more from the reference value of 1000 W/m² than the distributions corresponding to the sunny days. A higher value of BF for cloudy days than that corresponding to the sunny days, apparently differs from the trend shown in Fig. 6, at least in the central hours of the day. The differences with respect to the value of BF calculated at STC can reach a maximum of 3.53%, which strangely corresponds to the measurements taken on sunny days.

This result is also noticeable considering the whole spectrum of the experimental campaign (“All days”), since its relative difference is better than the calculated for sunny days because the cloudy days represent

Table 5
Power Bifaciality coefficient results at Operating Test Conditions.

	Average Values		Median Values	
	OperatingPower Bifaciality $\rho_{PM,OTC}$	Differences with calculated $\rho_{PM,STC}$	OperatingPower Bifaciality $\rho_{PM,OTC}$	Differences with calculated $\rho_{PM,STC}$
All days	0.799	-2.06%	0.814	-0.17%
Sunny days	0.787	-3.53%	0.816	0.08%
Partially overcast days	0.788	-3.36%	0.810	-0.69%
Cloudy days	0.812	-0.39%	0.815	-0.07%

almost 46% of the experimental campaign, compared to 33% of the sunny ones.

In order to eliminate extreme measurements that could distort the results, as they correspond to average calculation, the median values, and their difference with respect to the bifaciality coefficient obtained under STC conditions, were also included in Table 5. In this analysis, the results get closer to $\rho_{PM,STC}$ from section 3.1.

Figs. 6–8 already predicted what the use of the median value demonstrated quantitatively: by the end of the day, and even after the removal of potential sunset-induced shadows on the test modules, distortions still manifest in the results of the bifaciality coefficient with respect to $\rho_{PM,STC}$. In a first approximation, these distortions are due to the losses corresponding to the angle of incidence (AOI) of the solar radiation on the surface of the modules. This effect implicitly results in a significant decrease in the level of the incident irradiance. In the experimental set-up, this effect is more relevant in the PV_rear module, as the frame may project shadows in the module’s perimeter cells, therefore it also may have an influence in the decrease of the bifaciality coefficient.

This effect is less pronounced on cloudy days because the predominant component of the solar radiation is diffuse, and therefore, the bifaciality drops due to the angle of incidence that are observed on sunny days do not appear. There are only a couple of exceptions (BF_cloudy days 2 and 3 from Fig. 8) and this is because some cloudy days become slightly sunnier in the final hours.

Therefore, the reduction in the relative differences with respect to $\rho_{PM,STC}$ are not as pronounced in the cloudy day measurements between the mean and median values, as Table 5 indicates. Nevertheless, the instability in the value of the bifacial coefficient seems to be more intense in the early and late hours of this type of day, and it apparently creates a certain upward trend in the average value of the bifaciality coefficient, which is discussed in Section 3.3.

For a more in-depth analysis of the AOI influence in the OTC bifaciality coefficient results, and to eliminate its effect, a time filter was applied to the measurements of the experimental campaign. Only the data recorded in the time window of the central hours of the day (12h–14h UTC+1) have been considered, and therefore any distortion that may have occurred as a result of the AOI of the solar radiation is minimised.

The results in Table 6 show that the relative differences with respect

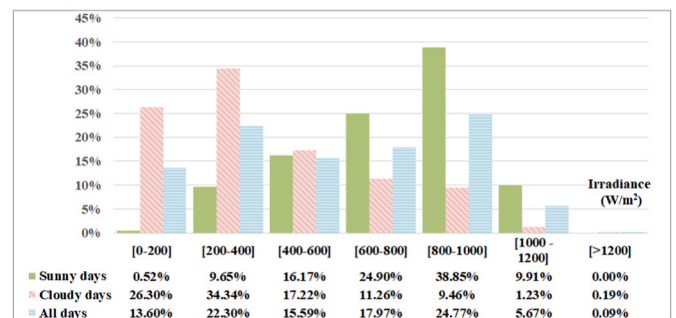


Fig. 9. Frequency distribution of the irradiance levels according to the different day types of the campaign.

to the values calculated under STC conditions are below 2% in all the scenarios. Therefore, the angle of incidence influences the results of the OTC bifaciality value. However, it should be noted that in all cases, the value of the bifaciality coefficient under real operating conditions is greater than the bifaciality coefficient under STC.

In this analysis, the explanation of the results also lies in the distribution of the irradiance values. Fig. 10 plots the frequency distribution of different irradiance ranges, but considering only the central hours of the day. It can be observed, mainly in the days classified as sunny and in the whole experimental campaign, that there is a portion of measurements that exceeds the reference threshold value of 1000 W/m², which causes this to be higher than the value of ρ_{Pm_STC} .

An additional column was included in Table 6 to assess the differences in the bifaciality factor considering the central hours of the day, with respect to the results shown in Table 5, which do not apply any temporal filter (with the exception of the edges of the day initially indicated). Hence, some of these differences are attributable to loss mechanisms that originate from the angle of incidence (AOI). It is observed that this effect is more predominant on sunny days than on cloudy ones.

In addition, these results also corroborate what is graphically represented in Fig. 6, since the value of the bifaciality coefficient is slightly lower (1.32%) for days classified as “cloudy” as for days classified as “sunny”.

3.3. – bifaciality coefficient dependence on the irradiance levels

The previous figures and tables show the results according to the temporal evolution of the bifaciality based on the proposed daily meteorological classification.

In the previous section, the AOI was found to have a negative influence on the values of the bifaciality coefficient. The higher the angle of incidence, the lower the value of in-plane-irradiance on the module. Therefore, some dependency on the irradiance levels was detected. In a preliminary analysis, it was observed that at lower irradiance levels (below the reference of 1000 W/m²), the bifaciality coefficient decreases.

However, and considering the frequency distributions analysed in Table 5 and Fig. 9, it is observed that for cloudy days, even though the irradiance distribution is significantly lower than the reference value of 1000 W/m², the relative difference of its operating power bifaciality with regards to the ρ_{Pm_STC} is not so large. This performance does not improve much either if the analysis is done only considering the central hours of the day, as Table 6 and Fig. 10 show. This fact may contradict the previous result that at lower irradiances, the bifaciality coefficient decreases.

Therefore, it is necessary to plot the variation of the operating bifaciality coefficient as a function of the irradiance values recorded. Fig. 11 shows this dependency taking into account the complete experimental campaign data set, where no time filter has been applied, except for the days’ tails. Therefore, these results include the distortion that occurs when the analysis is done beyond the central hours of the day, due to the angle of incidence losses (lower irradiance values) described in the

Table 6
Power Bifaciality coefficient average results at OTC considering the central hours of the day.

	OperatingPower Bifaciality ρ_{Pm_OTC}	Differences with calculated ρ_{Pm_STC}	Differences with average ρ_{Pm_OTC} (Table 5)
All days	0.825	1.12%	3.24%
Sunny days	0.831	1.87%	5.59%
Partially overcast days	0.825	1.18%	4.70%
Cloudy days	0.820	0.54%	0.93%

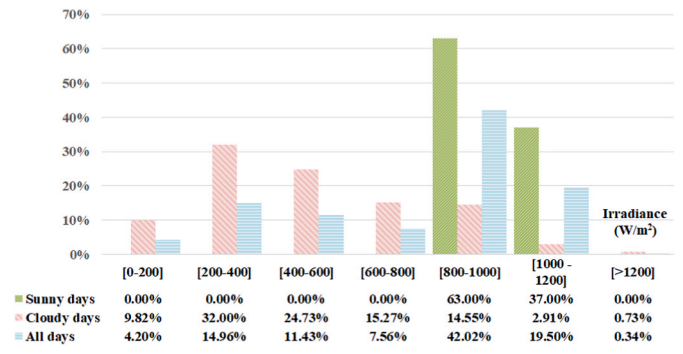


Fig. 10. Frequency distribution of irradiance levels according to the different day types considering only the daily central hours.

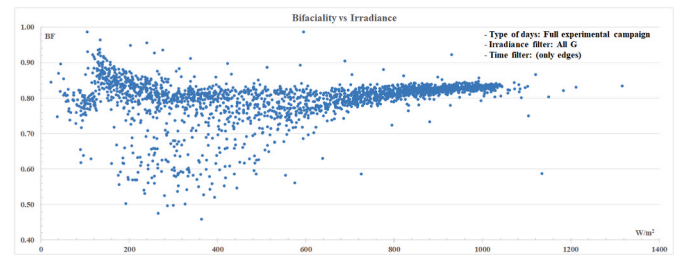


Fig. 11. Bifaciality coefficient as a function of the irradiance values.

previous section.

This figure shows that above 800 W/m², there is a greater accumulation of measured data, with a linear trend showing an almost constant value for the operational bifaciality coefficient.

This graphical representation also indicates another remarkable result. For irradiances below 600 W/m², there is a greater dispersion in the measured data. However, below irradiance levels of 400 W/m², it is especially noticeable that the variability of the bifaciality coefficient as a function of the irradiance does not follow a linear trend. If the analysis is done to values below 200 W/m², the trend is reversed, i.e., the lower the irradiance levels, the higher the bifaciality coefficient values. This result may prove what the manufacturer indicates in the technical data sheet of the module about the average relative efficiency reduction of 1.9%. Therefore, within this range of irradiance levels, the photovoltaic module no longer has a linear performance.

Therefore, if at low irradiance values, the bifaciality coefficient increases significantly more than at higher irradiance levels, this result may conflict with the preliminary conclusion discussed in Fig. 6 and Table 6, where it was found that the bifaciality coefficient in cloudy days was lower than that corresponding to sunny ones.

In order to solve this apparent inconsistency, the first step was to analyse the measured data by discriminating the effects that can be attributed to the angle of incidence. Fig. 12 includes a representation of the dependence of the bifaciality coefficient on the irradiance levels, but

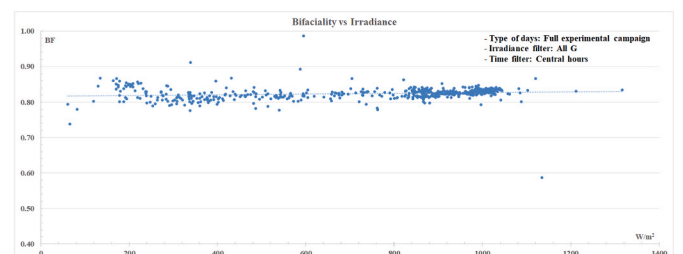


Fig. 12. Bifaciality coefficient as a function of the irradiance values only at the central hours of the day.

focusing only on the central hours of the days under analysis. The median value of the bifaciality coefficient obtained, considering only this set of data, is 0.826.

Fig. 12 also shows that above 800 W/m², there is a greater accumulation of measured data. Below this threshold value, the dispersion of the measurements is greater and the effect of irradiance values below 200 W/m² is almost non-existent. Therefore, at central hours, the predominant effect in the variation of the bifaciality coefficient is its linear dependency on the irradiance values.

If this analysis is complemented with the irradiance frequency distribution shown in Fig. 10, several aspects can be identified. On the one hand, if the entire experimental campaign and only the central hours of the day are considered, 61.5% of the measurements are recorded when the irradiance values are greater than 800 W/m², while only 4% of the data are accumulated in irradiances below 200 W/m². Therefore, $\rho_{PM,OTC}$ is close to that measured under STC conditions, and the effect of the reduction in relative efficiency at very low irradiance levels, indicated by the manufacturer, does not appear.

On the other hand, if we differentiate between groupings of sunny and cloudy days, we can see that in the first type of days, 100% of the data corresponds to values greater than 800 W/m². In the case of cloudy days, 54.5% of the values are contained within an irradiance range of 400–1000 W/m².

This makes the result of the decrease in $\rho_{PM,OTC}$ value seen in Fig. 11 consistent with the results of Figs. 6–8, and Tables 5 and 6, i.e., days whose irradiance levels are between 400 and 1000 W/m², as in the case of cloudy days, their bifaciality coefficient will be slightly lower than days whose irradiance distribution is closer to (or above) 1000 W/m². In addition, in the cloudy days’ scenario, the increase of the bifaciality coefficient at very low irradiance values has no effect on these measurements.

However, by observing again at Fig. 6, and to a lesser extent at Figs. 7 and 8, a source of discrepancy seems to remain. If at irradiance levels between 1000 and 400 W/m², the value of the bifaciality coefficient decreases, the measurements recorded in the afternoon (from 15:30 onwards) do not seem to follow this trend, as for sunny days, the value of the bifaciality coefficient decreases much more for sunny days than for cloudy ones.

To eliminate any doubt, the frequency distribution for the measurements made in the afternoon is plotted in Fig. 13, differentiating between sunny and cloudy days. In this case, it can be seen that 68% of the measurements for sunny days fall in the 400–800 W/m² irradiance range (98% if the range is taken as from 200 W/m²) and that there are no measurements above 800 W/m². This may explain the decreasing trend in the bifaciality coefficient.

On the other hand, if we focus on cloudy days, 35% of the afternoon measurements fall in the range 0–200 W/m² (this value rises to 88% if the range 0–400 W/m² is taken). Therefore, the predominant effect is that at low irradiance levels, the nonlinearity (reduction of relative efficiency) indicated by the manufacturer occurs.

This fact is already shown in Fig. 11, where the bifaciality coefficient

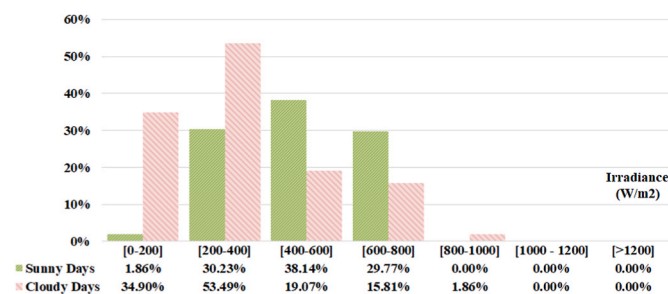


Fig. 13. Frequency distribution of the irradiance levels recorded in the afternoon (after 15:30h).

rises, even exceeding the average value measured for this type of day, and it is higher than that corresponding to sunny days, taking into account the afternoon time range.

This result also justifies the trend shown in Fig. 8, where it is observed that there is greater instability (greater amplitude) in the values of the bifaciality coefficient at the extremes of cloudy days, and therefore a higher mean value, as a result of the existence of low irradiance levels within the zone of nonlinear PV performance.

4. Conclusions and limitations of this study

In the light of the results obtained, the power bifaciality coefficient of a photovoltaic module, measured experimentally in real operating conditions and translated to STC, matches relatively well the value indicated by the manufacturer in its datasheet. Differences of 0.5% between the translated values and the indicated in the datasheet are obtained. This fact is a priori an indication of the suitability of the experimental campaign carried out. It also proves the feasibility of the proposed method for the outdoors evaluation of the bifaciality coefficient of a batch of photovoltaic modules. Additionally, it could be concluded that it is also an indication of the good manufacturing quality controls that the modules currently undergo.

According to the results, the maximum power bifaciality factor measured under real operating conditions but translated to STC remains practically constant regardless of the existing meteorological variability in which the measurements were recorded. Nevertheless, it is suggested that the measurements to be translated to STC should be carried out on completely sunny days since this improves the linear correlation coefficient, from R² = 0.816 corresponding to cloudy days, to R² = 0.994 from these sunny days according to the results obtained during the duration of the experimental campaign.

However, the maximum power bifaciality factor, measured under real operating conditions, differs from the idealistic values indicated by the manufacturer under STC, as it should be expected. These differences are dependent on the sort of days considered for the OTC versus STC comparison, i.e., sunny vs. cloudy days. Therefore, different bifaciality coefficient values are obtained for sunny or cloudy days. Overall, the bifaciality coefficient corresponding to sunny days is greater than the resulting from cloudy days, where $\rho_{PM,OTC}$ of 0.831 and 0.82 were calculated respectively. This means a difference of 1.87% and 0.54% from $\rho_{PM,STC}$ respectively.

The reasons for which the value obtained for sunny days is higher than that corresponding to STC conditions is due to the fact that the incident irradiance recordings were slightly higher than the reference used at STC ($G = 1000 \text{ W/m}^2$). Therefore, it is found that the bifaciality coefficient increases when the irradiance increases. This result is consistent with previously published research for indoor characterization (Bai et al., 2021). In an analogous manner, in the range of irradiances between 400 and 1000 W/m², there is a roughly linear decrease in the value of the bifaciality coefficient, which explains the lower average values on cloudy days compared to sunny ones.

Nevertheless, this conclusion do not remain valid throughout the daily evolution. During the central hours of the day, the bifaciality coefficient corresponding to sunny days is greater than the one obtained for cloudy days. However, at sunset, the bifaciality measured for sunny days dramatically drops, and the value of the bifaciality coefficient for cloudy days at this point of the day (sunset) exceeds that for sunny days. For this reason, if the average value is considered for the bifaciality assessment and comparison, the opposite conclusion according to the sunny vs. cloudy days may be obtained. There are differences of -3.53% and -0.39% with respect to $\rho_{PM,STC}$ respectively.

This result, and the fact that for cloudy days, the mean value of bifaciality is closer to that corresponding to STC than the values for sunny days, is explained by the occurrence of two effects that distort the results.

On the one hand, throughout the course of the day, the increase in

the angle of incidence (AOI) has a negative effect, which is more pronounced on sunny days than on cloudy days, because the predominant radiation component is diffuse on this type of days, and therefore, the AOI effect is suppressed. This causes the bifaciality coefficient to be higher on cloudy days than on sunny days in this time slot (sunset).

The second effect that may distort the result is related to the apparent increase that the bifaciality coefficient undergoes throughout the course of cloudy days. It can be observed that this value increases in the final hours of such days with respect to the central hours. This is explained by the non-linearity performance of photovoltaic modules at low irradiances. In this case, irradiances below 200 W/m^2 causes a non-linear increase effect in the bifaciality coefficient, which, added to the effect of the AOI previously mentioned, causes the value of ρ_{PM_OTC} to be higher on cloudy days than on sunny days in this time slot.

It is therefore concluded that on cloudy days, the predominant effect in the evening hours is the low irradiance levels that cause slight increases in the bifaciality, while on sunny days, the predominant effect is the AOI, which causes decreases in the bifaciality value.

To conclude, it is recommended that the assessment of the bifaciality coefficient be carried out in the central hours of the day, and preferably on sunny days.

4.1. – Limitations of this study

These results can be of special relevance taking into account that in real operating conditions, the rear side of the bifacial modules will be operating at relatively low irradiance levels, so to overcome the limitation of this study, it is considered necessary to extend this measurement campaign, but positioning the rear face of the modified module in its natural position, in order to identify, with greater accuracy, the effect that low irradiance levels have directly on its operation, as well as the view factor, which also affects the available incident irradiance on the rear side.

Moreover, these results can also be of interest in combination with studies regarding view factor modelling (Arias-Rosales and LeDuc, 2020), as well as to develop models of the performance of bifacial modules, taking into account not only the electrical and thermal effects, but also those corresponding to the optical influence (Gu et al., 2020).

Another limitation detected could be related to the duration of the experimental campaign. However, as the measurements approach the summer or the winter months, the combined comparison between sunny and cloudy days within the same recording period is reduced. In any case, it could be of interest to compare the performance of the BF between the winter and summer months.

While this study identifies the angle of incidence as a contributing factor to the results, it does not address the spectral distribution or its potential impact on the measurements. Hence, it is suggested to consider this variable in future analyses.

Funding

This work has been possible thanks to the project “Demo_BI-FV: Development of Advanced Models for the characterization of bifacial photovoltaic systems (PID2021-124161OB-I00)” funded by the Spanish Ministry of Science and the State Innovation Agency within the European Regional Development Fund (MCIN/AEI/10.13039/501100011033/FEDER, UE). The work of Jonathan Leloux was partially funded by the European Commission through the Horizon 2020 project SERENDI-PV (<https://serendipv.eu/>), which belongs to the Research and Innovation Programme, under Grant Agreement 953016. The work of David Moser was partially funded by the European Commission through the Horizon 2020 project TRUST-PV, which belongs to the Research and Innovation Programme, under Grant Agreement 952957

Declaration of competing interest

The authors declare that they have no known competing financial interests or personal relationships that could have appeared to influence the work reported in this paper.

Data availability

The data that has been used is confidential.

Acknowledgements

The bifacial research line developed by the corresponding author and principal co-investigator of the previously mentioned R&D project, was originated in a research internship done at the EURAC research centre under the Short Term Scientific Mission activity funded by the Cost action: PEARL PV: Performance and Reliability of Photovoltaic Systems: Evaluations of Large-Scale Monitoring Data (CA16235).

Index of notations and abbreviations

AOI	Angle of incidence
BF	bifaciality coefficient (referred to Pm)
BFPV	Bifacial photovoltaic
BNPI	Bifacial Nameplate Irradiance
BSI	Bifacial Stress Irradiance
BSTC	Bifacial Standard Test Conditions
G	Irradiance (W/m^2)
G_{STC}	Irradiance at STC ($G_{STC} = 1000 \text{ W/m}^2$)
I_{mpp}	Current at Pm (A)
$I_{mpp_{BSTC}}$	Current at Pm _{BSTC} (A)
I_{sc}	Short-Circuit Current (A)
$I_{sc_{BSTC}}$	Short-Circuit Current at BSTC (A)
OTC	Operating test conditions
P_m	Peak Power or Operating Power (W)
$P_{m_{BSTC}}$	Maximum power at Bifacial Standard Test Conditions
$P_{m_{STC}}$	Maximum power at Standard Test Conditions
POA	In-plane irradiance (W/m^2)
PV	Photovoltaic
STC	Standard Test Conditions
T_c	Cell's temperature ($^{\circ}\text{C}$)
$T_{c_{STC}}$	Cell's temperature at STC ($T_{c_{STC}} = 25 \text{ }^{\circ}\text{C}$)
V_{mpp}	Voltage at Pm (V)
$V_{mpp_{BSTC}}$	Voltage at Pm _{BSTC} (V)
V_{oc}	Open-Circuit Voltage (V)
$V_{oc_{BSTC}}$	Open-Circuit Voltage at BSTC (V)
ρ_{Pm_OTC}	Operating Power Bifaciality
ρ_{Pm_STC}	Maximum power bifaciality coefficient at STC
φ_{Isc}	Bifaciality coefficient of I_{sc}
φ_{Pm}	Bifaciality coefficient of Pm
φ_{Voc}	Bifaciality coefficient of V_{oc}

References

- Angulo, J.R., Calsi, B.X., Conde, L.A., Guerra, J.A., Muñoz, E., de la Casa, J., Töfflinger, J.A., 2022. Estimation of the effective nominal power of a photovoltaic generator under non-ideal operating conditions. *Sol. Energy* 231, 784–792. <https://doi.org/10.1016/j.solener.2021.12.015>.
- Arias-Rosales, A., LeDuc, P.R., 2020. Comparing View Factor modeling frameworks for the estimation of incident solar energy. *Appl. Energy* 277, 115510. <https://doi.org/10.1016/j.apenergy.2020.115510>.
- Bai, Q., Tian, H., Nan, C., Ouyang, L., Zhang, Y., Ma, J., Mao, S., Han, H., Yang, H., Wang, H., 2021. Investigation on bifaciality factor and ideality factor of PERC bifacial solar module under different irradiances. *Conf. Rec. IEEE Photovolt. Spec. Conf.* 248–251. <https://doi.org/10.1109/PVSC43889.2021.9518575>.
- Chudinzow, D., Nagel, S., Giselewski, J., Eltrop, L., 2020. Vertical bifacial photovoltaics – a complementary technology for the European electricity supply? *Appl. Energy* 264, 114782. <https://doi.org/10.1016/j.apenergy.2020.114782>.

- Cuevas, A., Luque, A., Eguren, J., del Alamo, J., 1982. 50 Per cent more output power from an albedo-collecting flat panel using bifacial solar cells. *Sol. Energy* 29, 419–420. [https://doi.org/10.1016/0038-092X\(82\)90078-0](https://doi.org/10.1016/0038-092X(82)90078-0).
- Eguren, J., Martínez-Moreno, F., Merodio, P., Lorenzo, E., 2022. First bifacial PV modules early 1983. *Sol. Energy* 243, 327–335. <https://doi.org/10.1016/j.solener.2022.08.002>.
- Gu, W., Ma, T., Li, M., Shen, L., Zhang, Y., 2020. A coupled optical-electrical-thermal model of the bifacial photovoltaic module. *Appl. Energy* 258, 114075. <https://doi.org/10.1016/j.apenergy.2019.114075>.
- Gu, W., Li, S., Liu, X., Chen, Z., Zhang, X., Ma, T., 2021. Experimental investigation of the bifacial photovoltaic module under real conditions. *Renew. Energy* 173, 1111–1122. <https://doi.org/10.1016/j.renene.2020.12.024>.
- Herrmann, W., Schweiger, M., Castro, J.B., 2017. Performance characteristics of bifacial PV modules and power labeling. In: 4th Bifi PV Workshop. Konstanz, Germany.
- IEA PVPS Task 13, 2021. Bifacial PV Modules & Systems Experience and Results from International Research and Pilot Applications, Performance, Operation and Reliability of Photovoltaic Systems.
- IEC) International Electrotechnical Commission, 2019. Photovoltaic Devices - Part 1-2: Measurement of Current-Voltage Characteristics of Bifacial Photovoltaic (PV) Devices. IEC TS 60904-1-2:2019.
- IEC) International Electrotechnical Commission, 2021a. Terrestrial Photovoltaic (PV) Modules - Design Qualification and Type Approval - Part 1: Test Requirements. IEC 61215-1:2021.
- IEC) International Electrotechnical Commission, 2021b. Terrestrial Photovoltaic (PV) Modules - Design Qualification and Type Approval - Part 1: Test Requirements. IEC 61215-2:2021 RLV.
- IEC) International Electrotechnical Commission, 2021c. Photovoltaic System Performance - Part 1: Monitoring. IEC 61724-1:2021.
- IEC) International Electrotechnical Commission, 2023. Photovoltaic Cells - Part 3: Measurement of Current-Voltage Characteristics of Bifacial Photovoltaic Cells. IEC TS 63202-3:2023.
- Katsikogiannis, O.A., Ziar, H., Isabella, O., 2022. Integration of bifacial photovoltaics in agrivoltaic systems: a synergistic design approach. *Appl. Energy* 309, 118475. <https://doi.org/10.1016/j.apenergy.2021.118475>.
- Kenny, O.P., Lopez-Garcia, J., Menendez, E.G., Haile, B., Shaw, D., Kenny, R.P., Lopez-Garcia, J., Menendez, E.G., Haile, B., Shaw, D., 2018. Characterizing bifacial modules in variable operating conditions. In: 2018 IEEE 7th World Conference on Photovoltaic Energy Conversion (WCPEC) (A Joint Conference of 45th IEEE PVSC, 28th PVSEC & 34th EU PVSEC). IEEE, pp. 1210–1214. <https://doi.org/10.1109/PVSC.2018.8547853>.
- King, D.L., Boyson, W.E., Kratochvil, J.A., W, B., Kratochvill, J., 2004. Photovoltaic Array Performance Model, Sandia Report No. 2004-3535. Sandia National Laboratories, Albuquerque, New Mexico.
- Libal, J., 2018. Chapter 6: impact of bifaciality on the leveled cost of PV-generated electricity. In: Bifacial Photovoltaics: Technology, Applications and Economics. Institution of Engineering and Technology, pp. 221–236. <https://doi.org/10.1049/PBPO107E.ch6>.
- Lopez-Garcia, J., Ozkalay, E., Kenny, R.P., Pinero-Prieto, L., Shaw, D., Pavanello, D., Sample, T., 2022. Implementation of the IEC TS 60904-1-2 measurement methods for bifacial silicon PV devices. *IEEE J. Photovoltaics* 12, 787–797. <https://doi.org/10.1109/JPHOTOV.2022.3161186>.
- Muehleisen, W., Loeschig, J., Feichtner, M., Burgers, A.R.R., Bende, E.E.E., Zamini, S., Yerasimou, Y., Kosel, J., Hirschl, C., Georgiou, G.E.E., 2021. Energy yield measurement of an elevated PV system on a white flat roof and a performance comparison of monofacial and bifacial modules. *Renew. Energy* 170, 613–619. <https://doi.org/10.1016/j.renene.2021.02.015>.
- Muñoz, J.V., Nofuentes, G., Fuentes, M., de la Casa, J., Aguilera, J., 2016. DC energy yield prediction in large monocrystalline and polycrystalline PV plants: time-domain integration of Osterwald's model. *Energy* 114, 951–960. <https://doi.org/10.1016/j.energy.2016.07.064>.
- Nordmann, T., Clavadetscher, L., 2004. PV on noise barriers. *Prog. Photovoltaics Res. Appl.* 12, 485–495. <https://doi.org/10.1002/ppp.566>.
- Patel, M.T., Ahmed, M.S., Imran, H., Butt, N.Z., Khan, M.R., Alam, M.A., 2021. Global analysis of next-generation utility-scale PV: tracking bifacial solar farms. *Appl. Energy* 290, 116478. <https://doi.org/10.1016/j.apenergy.2021.116478>.
- Riaz, M.H., Imran, H., Younas, R., Butt, N.Z., 2021. The optimization of vertical bifacial photovoltaic farms for efficient agrivoltaic systems. *Sol. Energy* 230, 1004–1012. <https://doi.org/10.1016/j.solener.2021.10.051>.
- Riedel-Lyngskaer, N., Petit, M., Berrian, D., Poulsen, P.B., Libal, J., Jakobsen, M.L., 2020. A spatial irradiance map measured on the rear side of a utility-scale horizontal single axis tracker with validation using open source tools. In: 2020 47th IEEE Photovoltaic Specialists Conference (PVSC). IEEE, pp. 1026–1032. <https://doi.org/10.1109/PVSC45281.2020.9300608>.
- Riedel-Lyngskær, N., Poulsen, P.B.P.B., Jakobsen, M.L.M.L., Nørgaard, P., Vedde, J., 2020. Value of bifacial photovoltaics used with highly reflective ground materials on single-axis trackers and fixed-tilt systems: a Danish case study. *IET Renew. Power Gener.* 14, 3946–3953. <https://doi.org/10.1049/iet-rpg.2020.0580>.
- Riedel-Lyngskar, N., Bartholomäus, M., Vedde, J., Poulsen, P.B., Spataru, S., 2022. Measuring irradiance with bifacial reference panels. *IEEE J. Photovoltaics* 12, 1324–1333. <https://doi.org/10.1109/JPHOTOV.2022.3201468>.
- Rodríguez-Gallegos, C.D., Liu, H., Gandhi, O., Singh, J.P., Krishnamurthy, V., Kumar, A., Stein, J.S., Wang, S., Li, L., Reindl, T., Peters, I.M., 2020. Global techno-economic performance of bifacial and tracking photovoltaic systems. *Joule* 4, 1514–1541. <https://doi.org/10.1016/j.joule.2020.05.005>.
- Tao, Y., Bai, J., Pachauri, R.K., Wang, Y., Li, J., Attaher, H.K., 2021. Parameterizing mismatch loss in bifacial photovoltaic modules with global deployment: a comprehensive study. *Appl. Energy* 303, 117636. <https://doi.org/10.1016/j.apenergy.2021.117636>.
- Tina, G.M., Bontempo Scavo, F., Merlo, L., Bizzarri, F., 2021a. Comparative analysis of monofacial and bifacial photovoltaic modules for floating power plants. *Appl. Energy* 281, 116084. <https://doi.org/10.1016/j.apenergy.2020.116084>.
- Tina, G.M., Scavo, F.B., Aneli, S., Gagliano, A., 2021b. Assessment of the electrical and thermal performances of building integrated bifacial photovoltaic modules. *J. Clean. Prod.* 313, 127906. <https://doi.org/10.1016/j.jclepro.2021.127906>.
- VDMA, 2022. International Technology Roadmap for Photovoltaic. 2021 Results.
- Vogt, M.R., Piliš, G., Zeman, M., Santbergen, R., Isabella, O., 2023. Developing an energy rating for bifacial photovoltaic modules. *Prog. Photovoltaics Res. Appl.* 1–12. <https://doi.org/10.1002/ppp.3678>.
- Yakubu, R.O., Mensah, L.D., Quansah, D.A., Adaramola, M.S., 2022. Improving solar photovoltaic installation energy yield using bifacial modules and tracking systems: an analytical approach. *Adv. Mech. Eng.* 14. <https://doi.org/10.1177/16878132221139714>.